High Temperatures – High Pressures, 2003/2004, volume 35/36, pages 237 – 249

DOI:10.1068/htjr098

# Carbon transport in diamond anvil cells

Vitali B Prakapenka, Guoyin Shen
Consortium for Advanced Radiation Sources (CARS), University of Chicago, Chicago, IL 60637, USA; fax: +1 630 252 0436; email: prakapenka@cars.uchicago.edu

Leonid S Dubrovinsky
Bayerisches Geoinstitut, Universität Bayreuth, D-95440 Bayreuth, Germany
Received 26 October 2002; in revised form 26 May 2003

**Abstract.** High-pressure-induced carbon transport from diamond anvils into the pressure chamber of diamond anvil cells (DACs) was studied by micro-Raman spectroscopy. Depending on experimental conditions (temperature and pressure), various carbon phases (amorphous carbon, diamond, microcrystalline or nanocrystalline graphite) were detected in the originally carbon-free samples. Temperature-induced growth of a graphite phase at the sample/diamond interface was observed in situ at high pressure in an externally heated DAC. In laser-heated samples inside the pressure-transmitting medium, at pressures above 6 GPa there was transport of carbon from the diamond culet surface into the heated part of the sample. These observations suggest that account should be taken of possible carbon diffusion in high-pressure research with DACs, such as high-pressure melting, element partitioning, phase transformations, chemical reactions, and electrical resistivity.

## 1 Introduction

The diamond anvil cell (DAC), in which two gem-quality diamonds apply a force to the sample, revolutionized high-pressure research. The DAC technique initiated in 1958 (Jamieson et al 1959; Weir et al 1959) allows the study of material properties by various methods, such as Mössbauer, infrared, and Raman spectroscopy; resistivity measurements; x-ray diffraction; and inelastic scattering (eg Eremets 1996). Heating of diamond-cell samples, with both resistance heaters and lasers, has extended attainable pressure – temperature conditions to those that prevail in most of the Earth's interior (Bassett 2001; Shen et al 2001).

A large number of new phase transitions and chemical reactions of different compounds at high pressures and high temperatures in DACs have been reported in the past three decades. However, element distribution in samples recovered from DACs has been poorly investigated owing to difficulties arising from the use of very small amounts of materials (typical diameter of the pressure chamber is 20 – 150 μm and its thickness is 5 – 50 μm). Nevertheless, even a small amount of impurities in the pressure chamber (eg oxygen, carbon, etc) could significantly change the chemical and physical properties of materials. Hence, experimental data from DAC studies, such as phase transformations and chemical reactions, partitioning, and melting temperatures, could be significantly affected by the involved impurities.

Diamond anvils are generally considered to be chemically inert and stable at high pressure (Bundy et al 1996). However, many investigators (Gogotsi et al 1999; Kailer et al 1999; Mao and Hemley 1991; Vohra and McCauley 1993) have observed stress-induced transformation of diamond to graphite or other phases even in the diamond stability range. Does the transformation occur in the highly stressed culet area of diamond anvils at high pressures? Is carbon diffusion involved in the sample chamber in a DAC at high pressures and high temperatures? The purpose of this paper is to answer these two questions. To study carbon distribution inside the pressure chamber of a DAC, we used micro-Raman spectroscopy, one of the best and most widely used techniques for the analysis of different carbon phases. Its spatial resolution with analyzed area down to

2 μm allows 'mapping' the distribution of Raman-active substances in the small pressure chamber of a DAC.

Carbon phases can be easily identified by Raman signals. The features of Raman spectra depend on the ratios of $sp^1$(polymer-like)/$sp^2$(graphite-like)/$sp^3$(diamond-like) bonds (Knight and White 1989). The visible (usually with an excitation laser with wavelength of 514.5 nm) Raman spectroscopy is 50 – 100 times more sensitive for $sp^2$ sites than those for $sp^3$ (Pickard et al 1998). Therefore, even a small amount of graphite phase can be detected with micro-Raman spectroscopy. Raman spectrum of diamond has strong $T_{2g}$ (1332 $cm^{-1}$) zone center mode. Natural single-crystal graphite shows intense sharp Raman mode at 1580 $cm^{-1}$ (G band) and weak one at 2724 $cm^{-1}$. the 1357 $cm^{-1}$ peak (D band) appears in the spectrum of polycrystalline graphite. The D/G intensity ratio, as well as precise wavelength of D and G bands, depend on a degree of disordering of carbon phases: crystalline or amorphous nature and size of crystal grains. It is known (Knight and White 1989) that features of Raman spectra of carbon phases depend on the synthesis method and conditions. According to Ferrari and Robertson (2000), at transformation of single-crystal graphite to nanocrystalline material, the G band moves from 1580 to ~1600 $cm^{-1}$, the D band appears, and the D/G intensity ratio increases. For amorphous carbon, the G band changes from 1600 to ~1500 $cm^{-1}$ with low D/G intensity ratio and broad G band (Ferrari and Robertson 2000).

## 2 Apparatus

Different carbon phases were observed in the quenched samples from a number of experiments conducted in the past few years. Several typical examples of those samples are described below. These samples were actually used for other studies such as for melting and phase transition. In addition, we performed a set of specially designed model experiments to confirm carbon transport inside samples in DAC at high pressures and high temperatures.

### 2.1 *High-pressure technique*

Three types of DACs [Mao – Bell, membrane DIA CELL, and flat four or three pins (designed in Tel Aviv University, TAU)] were used in experiments. Type I and type II brilliant cut diamond anvils with 250 – 350 μm culets were used. Holes 100 – 130 μm in diameter were drilled in the 300 or 150 μm thick stainless steel, or in 250 μm thick rhenium gaskets pre-indented to a thickness of 30 to 90 μm. Pressure was measured by ruby fluorescence scale or by using equation of state of Au, Pt, or NaCl.

### 2.2 *Heating systems*

We used heating facilities at Uppsala Lab (Sweden), European Synchrotron Radiation Facility (ESRF, Grenoble, France), and Advanced Photon Source (APS) at Argonne National Laboratory (Chicago, USA).

At Uppsala Lab (Dubrovinsky and Saxena 1999) the laser-heating system with Nd – YAG laser ($\lambda = 1064$ nm, 30 W) makes it possible to heat samples with controllable temperatures up to 3000 K. Laser-heating spot of 10 – 20 μm was scanned on selected areas of samples.

The laser heating at ESRF was carried out with a Nd:YAG laser ($\lambda = 1064$ nm, 17 W). Temperatures between 1300 K and 1700 K were estimated by colors of the heating spot.

At APS, a double-sided laser-heating technique with a laser spot of 20 – 40 μm was employed. The temperature was measured from thermal radiation (Shen et al 2001).

External ceramic heating assemblage was used for heating TAU type DAC (Pasternak et al 1999). The entire cell was placed inside the heater. To protect diamond anvils and metal body of the cell, the heating system was filled with inert gas ($Ar + 2\%H_2$ mixture). Constantan wire was used for the heater. A type K thermocouple was attached

to the diamond anvil – gasket interface inside the heater and used for temperature measurements.

2.3 *Analytical technique*

Raman spectra were collected with an InstaSpec-IV CCD detector with a MultiSpec-257 imaging spectrograph (grating 1200/350). Confocal micro-optical systems in a backscattering geometry with focus depth of 2 – 5 μm were used. For Raman excitation we chose the green line of an argon laser ($\lambda = 514.53$ nm). Output power of the laser beam varied in the range of 100 – 350 mW and focused on a spot about 6 μm in diameter on the sample. Raman scattering was recorded in the spectral range 180 – 2800 $cm^{-1}$ with a resolution of 4 $cm^{-1}$ (Prokopenko et al 2001). The quenched samples (recovered samples outside the DAC) were also analyzed with a Renishaw Raman 2000 spectrometer with output green laser power 50 mW and resolution of 2 $cm^{-1}$. A Raman system installed at the GeoSoilEnviroCARS at the APS was used for some recent samples. All Raman spectra were collected on quenched samples outside DAC (except one in-situ study on $TiO_2$). In all model experiments, quenched samples were analyzed by Raman spectroscopy immediately after opening the cell, while the remaining samples were kept in evacuated desiccators before analysis.

## 3 Samples

All samples used in high-pressure experiments were of high purity and no carbon phases or hydrocarbon compounds were detected by Raman spectroscopy. Further confirmation was made for some of the samples by IR spectroscopy.

3.1 *High-pressure samples at ambient temperature*

A number of samples were prepared by compression at ambient temperature in a DAC (table 1).

The cristobalite phase of $SiO_2$ (#1) was formed after annealing of high purity sol – gel glass at 1800 K for 15 min and then grinding to obtain a microcrystalline powder with particle size of about 1 μm. The membrane type of DAC was used for high-pressure generation up to 56 GPa and then recovered to ambient pressure (Prokopenko et al 2001).

Iron – nickel alloy (#2) was synthesized by arc-melting in an argon atmosphere; its composition was $Fe_{55}Ni_{45}$ (Dubrovinsky et al 2001). A peak pressure of 60 GPa was achieved in the DAC.

Pure α-quartz phase of $GeO_2$ (#3) powder (Aldrich Inc., 99.9999%) together with gold wire (Goodfellow Inc., 99.99+%) of 5 μm diameter (used as pressure calibrant) was pressurized up to 48 GPa in a 4-pin flat DAC.

No pressure medium was used for all these runs.

3.2 *High-pressure – high-temperature samples (laser heated)*

$Fe_{0.5}Mg_{0.5}O$ and $SiO_2$ mixture in 1:1 ratio was loaded in an argon atmosphere in a piston–cylinder type small DAC. At different pressures [75 GPa (#4) and 45 GPa (#5)], the samples were laser heated at 2000 (100) K with the double-sided laser-heating system at APS.

A powder disc of $Rh_2O_3$ (Aldrich Inc., 99.8%) embedded in NaCl pressure medium in Mao – Bell DAC was laser heated at 60 GPa at ESRF (#6).

A powder disc of $Fe_3O_4$ (#7) was loaded in Mao – Bell DAC in inert atmosphere (argon) inside a CsCl pressure-medium-like sandwich (Pasternak et al 1999). The sample at 75 GPa was laser heated at temperatures between 1800 and 2200 K.

Glass with the composition $MgSiO_3$(90%) – $Al_2O_3$(10%) was mixed with platinum powder (Goodfellow Inc., 99.95%) in a volume proportion ~10:1 (#8). The laser heating was carried out at 1500 (100) K from both sides at 45 GPa at ESRF.

**Table 1.** Selected samples and their conditions reported in this study (numbers in parenthesis denote uncertainties in measurements).

| No (#) | Precursor | Pressure-transmitting medium | DAC | Peak pressure/GPa | Pressure calibrant, method | Peak temperature/K | Type of heating | Observed carbon phase |
|---|---|---|---|---|---|---|---|---|
| 1 | cristobalite phase of $SiO_2$ | no | Mao – Bell cell | 56(1) | Au, x-ray | 300 | – | microcrystalline graphite |
| 2 | $Fe_{55}Ni_{45}$ | no | 4-pin cell | 60(2) | ruby, fluorescence | 300 | – | microcrystalline graphite |
| 3 | α-quartz phase of $GeO_2$ | no | 4-pin cell | 48(1) | Au, x-ray | 300 | – | microcrystalline graphite |
| 4 | $Fe_{0.5}Mg_{0.5}O$ and $SiO_2$ mixture | no | small piston – cylinder | 75(3) | $Fe_{0.5}Mg_{0.5}O$, x-ray | 2000(100) | double side laser heating, APS | microcrystalline graphite |
| 5 | $Fe_{0.5}Mg_{0.5}O$ and $SiO_2$ mixture | no | small piston – cylinder | 45(2) | $Fe_{0.5}Mg_{0.5}O$, x-ray | 2000(100) | double side laser heating, APS | diamond |
| 6 | $Rh_2O_3$ inside NaCl | NaCl | Mao – Bell cell | 60(2) | NaCl, x-ray | 1500(200) | laser heating, ESRF | nanocrystalline graphite |
| 7 | $Fe_3O_4$ inside CsCl | CsCl | Mao – Bell cell | 75(2) | CsCl, x-ray | 2000(100) | laser heating, Uppsala | micrographite and diamond |
| 8 | $MgSiO_3$(90%) – $Al_2O_3$(10%) glass plus Pt | no | 4-pin cell | 45(1) | Pt, x-ray | 1500(200) | laser heating, ESRF | diamond |
| 9 | Fe inside $SiO_2$ | $SiO_2$ | 4-pin cell | 125(5) | ruby, fluorescence | 2300(100) at 90 GPa | laser heating, Uppsala | micrographite and diamond |
| 10 | Rutile phase of $TiO_2$ | no | TAU cell | 52(2) | ruby, fluorescence | 850(10) | external electrical heating, Uppsala | micrographite, amorphous |
| 11 | Fe inside NaCl | NaCl | 4-pin cell | 6(1) | ruby, fluorescence | 1700(100) | laser heating, Uppsala | microcrystalline graphite |
| 12 | Fe inside KCl | KCl | 4-pin cell | 10(1) | ruby, fluorescence | 1700(100) | laser heating, Uppsala | microcrystalline graphite |
| 13 | Cu inside NaCl | NaCl | 4-pin cell | 18(1) | ruby, fluorescence | 1700(100) | laser heating, Uppsala | micrographite and diamond |
| 14 | Fe inside KCl | KCl | 4-pin cell | 6(1) | ruby, fluorescence | 1700(100) | laser heating, Uppsala | microcrystalline graphite |
| 15 | Fe inside NaCl | NaCl | 4-pin cell | 16(2) | ruby, fluorescence | 710(10) | external electrical heating, Uppsala | microcrystalline graphite |

An iron foil (Goodfellow Inc., purity 99.99+%) was placed between two layers of cristobalite in a DAC (#9). The laser heating was carried out at a maximum pressure of 90 GPa at 2300 (100) K from both sides. After heating, the pressure was increased to 125 GPa, and then released to ambient pressure.

Duration time of laser heating at one point for all samples in DAC was more than 5 min.

3.3 *High-pressure – high-temperature samples (electrically heated)*
Pure powder of rutile phase of $TiO_2$ (#10) was pressurized in a TAU-type cell (Pasternak et al 1999). Small ruby chips were used for pressure measurements at ambient and elevated temperatures (Rekhi et al 1999). At each pressure step (15, 32, 48, and 52 GPa) heating – cooling cycles were repeated. The Raman spectra were collected for samples in-situ at high pressures and high temperatures and for a quenched sample outside the cell as well.

3.4 *Model experiments*
Pieces of iron wire 25 μm in diameter (Goodfellow Inc., purity 99.99+%) or copper wire 10 μm in diameter (Goodfellow Inc., purity 99.99%) were placed between two layers of pressure-transmitting medium (#11 – #15), NaCl or KCl (figure 1). The halides are transparent in visible and near IR and this allowed us to heat metals with Nd : YAG laser and perform Raman measurements. Both NaCl and KCl were heated at 420 K overnight before loading in the cell. The loading was done in an argon atmosphere.

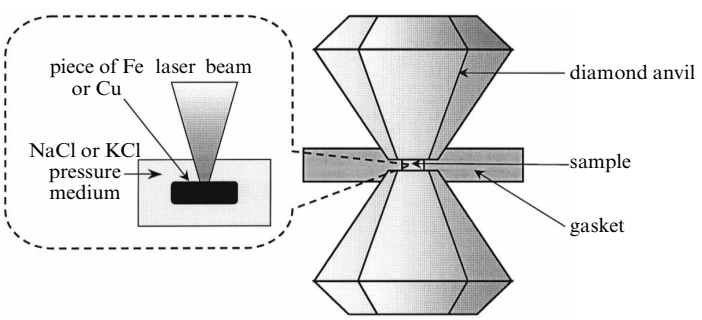


**Figure 1**. Sample configuration for high-temperature model experiments using laser-heating technique.

At pressures of 6, 10, or 18 GPa, samples (#11 – #14) were heated for 5 – 10 min by Nd : YAG laser focused on a spot about 20 μm in diameter on the metal surface. The temperature in the center of the laser spot was 1700 (100) K. Sample #15 was heated at 710 (10) K for 30 min at 16 GPa in an externally heated DAC. After analysis of quenched samples outside DAC, NaCl or KCl was removed by etching in distilled water and Raman spectra were collected directly from the metal surface of the quenched products.

## 4 Results

Figure 2 shows the Raman spectra recorded outside DAC for different materials pressurized above 45 GPa and heat-treated with Nd : YAG laser at temperatures above 1500 K. The carbon phases listed below were observed in the originally carbon-free samples.

Raman spectra collected from a mixture of $Fe_{0.5}Mg_{0.5}O$ and $SiO_2$ (#4) after laser heating of the sample at 75 GPa in DAC (figures 2a and 2b) contained the D and G bands at 1375 $cm^{-1}$ and 1600 $cm^{-1}$ or 1356 $cm^{-1}$ and 1605 $cm^{-1}$. According to Ferrari and Robertson (2000) these Raman spectra correspond to microcrystalline graphite. Nanocrystalline carbon with broad Raman bands at 1338 $cm^{-1}$ and 1593 $cm^{-1}$ was observed in the mixture of $Rh_2O_3$ and NaCl powders (#6) after laser heating at the peak pressure of

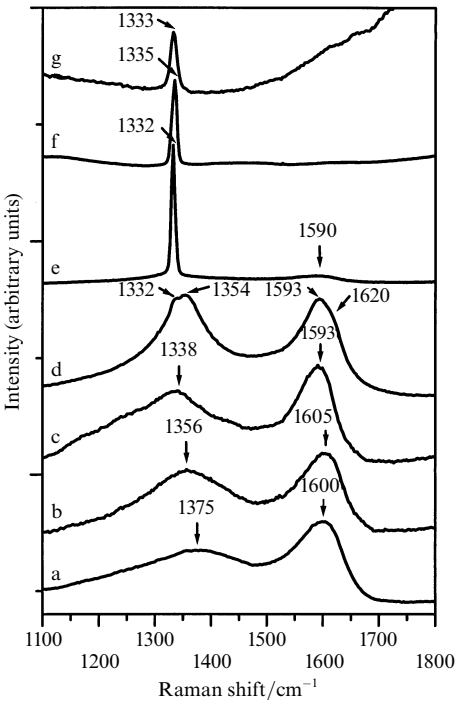


**Figure 2.** Raman spectra of various quenched samples compressed to different peak pressures and heated by a Nd:YAG laser beam at temperatures above 1500 K. Several carbon phases were observed, depending on sample history. Sample numbers are from table 1. a and b—mixture of $Fe_{0.5}Mg_{0.5}O$ with $SiO_2$ (cristobalite) in the ratio 1:1, peak pressure 75 GPa, various locations (#4); c—mixture of $Rh_2O_3$ with NaCl powder, peak pressure 60 GPa (#6); d and e—$Fe_3O_4$ sandwiched in CsCl pressure medium, peak pressure 75 GPa, various locations (#7); f—mixture of $Fe_{0.5}Mg_{0.5}O$ and $SiO_2$ (cristobalite) in the ratio 1:1, peak pressure 45 GPa (#5); g—mixture of $MgSiO_3$(90%) – $Al_2O_3$(10%) glass with Pt powder, peak pressure 45 GPa (#8).

60 GPa (figure 2c). A number of micrographite phases and diamond were formed in $Fe_3O_4$ inside CsCl (#7) after laser heating at 75 GPa (figures 2d and 2e). Only the diamond phase with Raman band positions at 1335 cm$^{-1}$ and 1333 cm$^{-1}$ was recorded for the mixture of $Fe_{0.5}Mg_{0.5}O$ and $SiO_2$ (#5, figure 2f) and for $MgSiO_3$(90%)–$Al_2O_3$(10%) glass mixed with platinum powder (#8, figure 2g), respectively, after laser heating at 45 GPa.

Diamond with Raman bands located between 1330 cm$^{-1}$ and 1335 cm$^{-1}$, and polycrystalline graphite phases of carbon were observed for iron ($SiO_2$ was used as the pressure medium) after laser heating at 30 GPa and 90 GPa and recovery from the peak pressure of 125 GPa (#9, figure 3).

Even at room temperature we have detected pressure-induced formation of microcrystalline graphite on samples with different chemical compositions loaded without a pressure medium (figure 4). For example, the starting material $GeO_2$ (#3) does not show any Raman bands of carbon phases (figure 4a). However, after recovery from 48 GPa, the sample of $GeO_2$ showed polycrystalline graphite phase with two intensive Raman modes at 1348 cm$^{-1}$ and 1585 cm$^{-1}$ (figure 4b and insert). After pressurizing $Fe_{55}Ni_{45}$ alloy (#2) to 60 GPa, two broad graphite bands were detected at 1335 cm$^{-1}$ and 1593 cm$^{-1}$ (figure 4b). The maxima of D and G modes at 1354 cm$^{-1}$ and 1600 cm$^{-1}$ were observed for the $SiO_2$ sample (#1) after recovery from 56 GPa (figure 4c). Such Raman features correspond to microcrystalline graphite with different grain sizes (Schindler and Vohra 1995).

Temperature-induced formation of carbon clusters was observed in-situ at high pressure in DAC for the $TiO_2$ sample (#10, figure 5). At pressures between 13 and 15 GPa we detected the appearance and growth of Raman bands of graphite at 1614 cm$^{-1}$ with temperature increasing from 300 K to 690 K. At the same time, broadening of the diamond Raman band at about 1360 cm$^{-1}$ was observed. After cooling to room temperature, the intensity of the G band did not change, but the position of the G line shifted to 1644 cm$^{-1}$ owing to changes of pressure and temperature. As the pressure increased to 32 GPa at room temperature the G band shifted from 1644 cm$^{-1}$ to 1695 cm$^{-1}$, getting broader and less intense. Subsequent heating to 710 K at that pressure

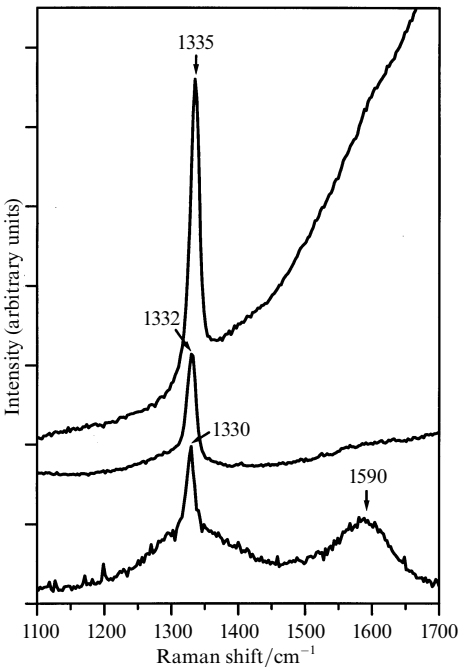


**Figure 3.** Raman spectra recorded at different points of the quenched sample of iron (inside $SiO_2$) after laser heating at 90 GPa and recovered from peak pressure of 125 GPa (# 9). The diamond and graphite phases or their mixture were observed in the same sample.

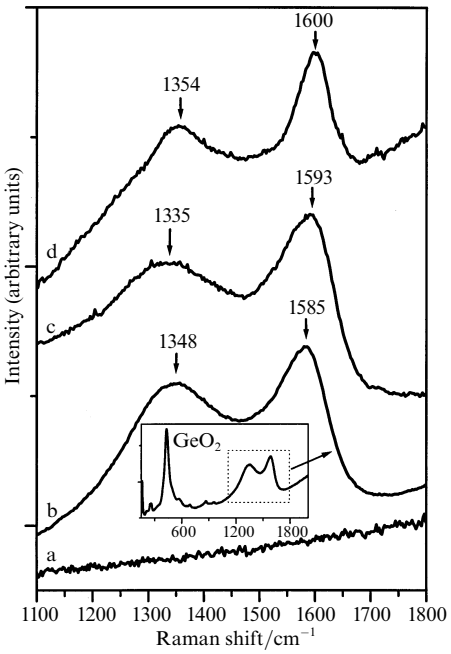


**Figure 4.** Raman spectra of quenched samples after compression at room temperature: a—starting material of $GeO_2$, b—$GeO_2$ recovered from 48 GPa (# 3), c—$Fe_{55}Ni_{45}$ after 60 GPa (# 2), d—$SiO_2$ (cristobalite) after compression to 56 GPa (# 1). The graphite phase was always observed with different starting materials.

slightly reduced the intensity of the graphite band. As the pressure increased to 52 GPa and on heating to 800 K, complete disappearance of graphite band was observed. On decompression at ambient temperature at 11 GPa the weak Raman band of graphite was detected again. After recovery of the sample outside the DAC at ambient conditions (figure 5), the amorphous carbon phase was found by Raman spectroscopy (Fominski et al 1993).

Confocal geometry of the Raman system allows significant reduction of scattering from the diamond anvil, which is very beneficial for collecting in-situ high-pressure data as a function of temperature from samples in DAC. For the in-situ experiment (#10), the maximum intensity of Raman graphite band was obtained from the focal spot position in the middle of the sample. The Raman signals of graphite phase completely disappeared at focal spot locations more than 10 μm away along the loading axis from the diamond/sample interface. The shift of graphite Raman peaks with pressure and the observation of carbon phase on the surface of quenched samples provide clear evidence that Raman signals come at least from the sample/diamond interface.

Do carbon phases appear only at the interface between the diamond anvil and the sample chamber? To answer this, we carried out a set of specially designed experiments. As described in section 2 and shown in figure 1, small pieces of iron or copper wires were placed inside NaCl or KCl to separate the metal from the diamond anvils. Such experimental arrangement allows us to collect Raman spectra (confocal setup) from the surface of the sample (from the diamond – sample interface) and from the surface of the metal inside NaCl or KCl. In addition, we performed Raman measurements after the recovery of metals with the pressure medium removed by etching with distilled water.

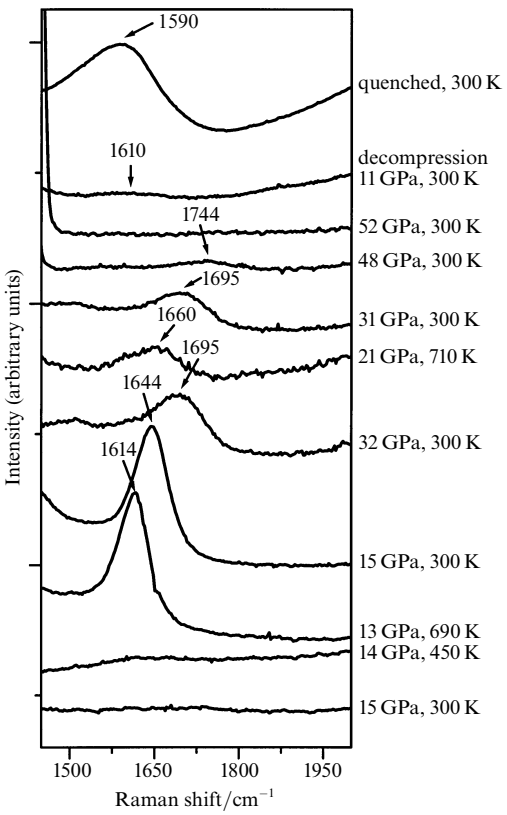


**Figure 5.** Raman spectra recorded in situ in a flat four-pin DAC for $TiO_2$ (starting material was carbon-free pure rutile) at different pressures and temperatures (# 10). The temperature-induced graphite phase formation was observed in situ in the DAC at pressures of about 15 GPa.

The Raman spectra collected from different spots of samples recovered after laser heating at different pressures are shown in figure 6. On all samples inside the pressure medium, graphite was observed clearly on laser-heated portions. In one case, where a portion of iron sample at 6 GPa (#11) was in contact with the diamond anvil and therefore was not heated by the laser, weak signals from graphite were detected (figure 6a). It is important to note that the intense Raman signals of microcrystalline graphite were observed for this sample (#11) on the iron surface, which was separated from diamond anvil by a layer of NaCl, both before (figure 6b) and after (figure 6c) dissolving the NaCl medium.

To estimate the concentration of graphite with depth, we measured intensities of Raman signals at different focal planes by keeping collection time constant (600 s). Raman spectra collected at the same lateral position on the surface of KCl and on the surface of iron inside KCl are shown in figures 6d and 6e, respectively, after the sample was laser-heated at 10 GPa (#12) and removed from DAC. Raman signal intensities suggest that the concentration of graphite increases with depth. For the unheated areas, however, we did not observe an increasing intensity of the G band with depth. The thickness of the KCl layer was about 20 – 25 μm, while the focus depth of our Raman system in confocal configuration was less than 5 μm.

Polycrystalline graphite and diamond were formed after laser heating of copper wire at 18 GPa (#13). The Raman spectra from the recovered sample, measured after removal of NaCl, clearly show the presence of a diamond band at 1332 cm$^{-1}$ (figure 6f) and microcrystalline graphite bands at 1355 cm$^{-1}$, 1585 cm$^{-1}$, and 1622 cm$^{-1}$ (figure 6g) on the copper wire.

The first-order and second-order Raman scattering of the carbon phase collected from the surface of iron inside KCl (#14) after laser heating at 6 GPa is shown as the insert in figure 6. The two sharp G and D Raman bands are located at 1590 cm$^{-1}$ and

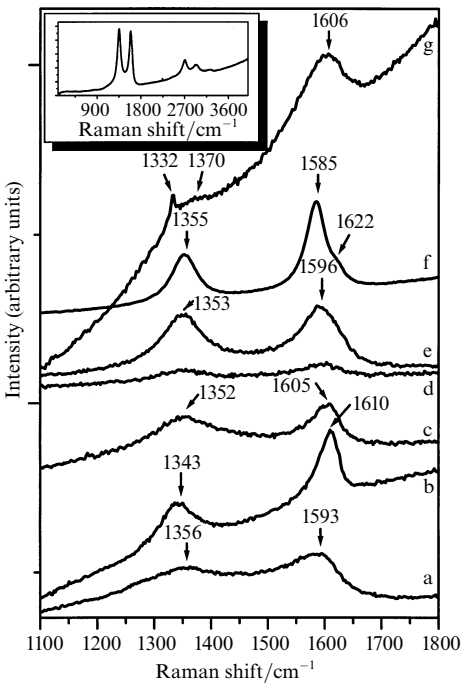


**Figure 6.** Raman spectra collected for samples specially designed for model experiments quenched from various peak pressures after laser heating at 1700 K: a and b—data collected from the surface of NaCl and iron sample that was touching the diamond anvil surface, respectively, quenched from 6 GPa (# 11); c—sample #11 after removal of NaCl by etching with distilled water; d and e—iron inside KCl, and the same points on the surface of KCl, quenched from 10 GPa (# 12); f and g—copper recovered from 18 GPa and after removal of NaCl, different locations (# 13). The insert shows the full Raman spectrum of graphite phase of carbon in a DAC for iron sample recovered from 6 GPa inside KCl (# 14).

1352 cm$^{-1}$, and weak broad bands are at 1090 cm$^{-1}$, 1620 cm$^{-1}$, 2700 cm$^{-1}$, 2937 cm$^{-1}$, 3223 cm$^{-1}$. Such features of the Raman spectrum correspond to polycrystalline graphite (Wilhelm et al 1998). No sign of Raman bands for iron or copper oxides was detected in any of the samples.

Note that the distribution of carbon in the high-pressure chamber is not uniform, especially for laser-heated samples. In some samples, Raman signals from carbon phases at one position could be significantly different from those in an area only about a few micrometers apart. This could be partly due to non-uniform pressure – temperature distribution and sample inhomogeneity. The other possible reason could be that carbon reacted with the sample forming Raman-inactive or low-scattering compounds. It is also possible that some parts of the samples were lost and their microstructure was disturbed during extraction from DAC.

Surfaces of diamond anvils before and after all experiments described above were carefully inspected under microscope and no visual defects and cracks were found. Raman spectroscopy shows diamond peaks only from anvil surfaces before the experiments (figure 7c). However, after most high-pressure experiments, on the culet surface of the diamond anvil a graphite phase could be observed with Raman features similar to those observed from the removed samples. For example, figure 7 shows the features of the graphite phase on the surface of iron (#15, figure 7a) and on the diamond anvil surface (figure 7b). However, after cleaning, the only diamond Raman band can be found on the surface of the diamond anvil (figure 7c).

Thus, we have demonstrated the following observations: Raman signals from carbon clusters were detected for all high-pressure samples recovered from DACs (runs #1 – 15); a thin layer on the culet surface of the diamond anvil (or the sample/diamond interface) was found to contain crystalline graphite phase at high-temperature – high-pressure experiments (runs #10 and 15); different carbon phases were observed on the surfaces of recovered samples which initially were separated from diamond anvils by various media in high-pressure – high-temperature experiments (runs #11 – 14).

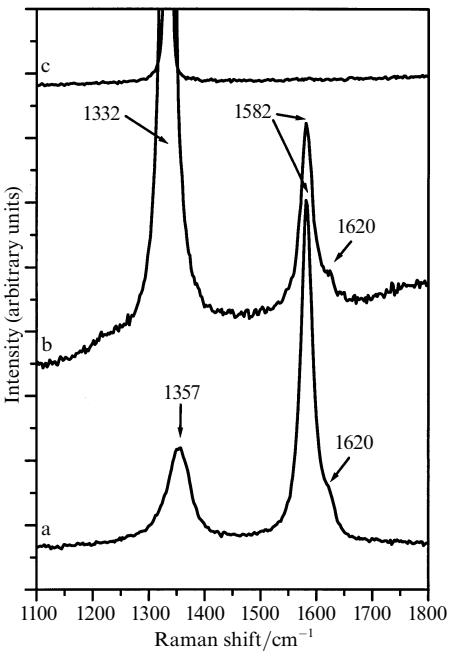


**Figure 7.** Raman spectra collected immediately after opening the DAC: a—surface of the iron piece inside NaCl after external heating at 710 K for 30 min at 16 GPa (# 15); b—surface of diamond culet after opening the DAC; c—surface of diamond culet after cleaning.

## 5 Discussion

All starting materials in our experiments were carbon-free and their Raman spectra showed no sign of contamination by any carbon phases. All heated samples were loaded in inert atmosphere. There is only one source of carbon—the diamond anvils. Diamond is the hardest known material. There should be no reversible phase transformation of cubic diamond structure to other phases at pressures above 6 GPa according to the high-pressure phase diagram (Bundy et al 1996). However, there are a few reports about a pressure-induced transformation of diamond to graphitic or other carbon phases under non-hydrostatic conditions (Gogotsi et al 1999; Kailer et al 1999; Mao and Hemley 1991; Vohra and McCauley 1993). The formation of lonsdaleite on the cut surfaces of diamond crystals and the formation of nanocrystalline graphite from the fracture of diamond under 300 GPa with a new Raman band at 1491 cm$^{-1}$ has been reported (Knight and White 1989; Vohra and McCauley 1993).

Taking into account available experimental data we propose the following explanation of the formation of carbon phase in DAC experiments (figure 8). The thin layer of the diamond culet surface is under high stress at high pressures and is transformed to amorphous or graphite phases. A layer of disordered carbon can then form at the interface between the diamond anvil and the sample (figures 4 and 7), providing a source for carbon diffusion. Weakly bonded carbon atoms in the disordered layer may help to initiate and further enhance the diffusion process. At room temperature and high pressure the diffusion process may be slow. Therefore, the graphite phase is found only on the surface of quenched samples after non-hydrostatic high-pressure experiments at room temperature (figure 4).

Upon heating, especially during laser heating, the diffusion rate and mobility of atoms increase as temperature, stresses, and temperature gradients increase (Lasaga 1998). As a result, amorphous carbon can form various clusters of crystalline carbon phases (figures 2, 3, 6, and 7) (Ree et al 1999). The process which lead to the formation of the crystalline carbon phases at high pressures and high temperatures, is not in equilibrium and we should not expect the formation of only thermodynamically stable phases

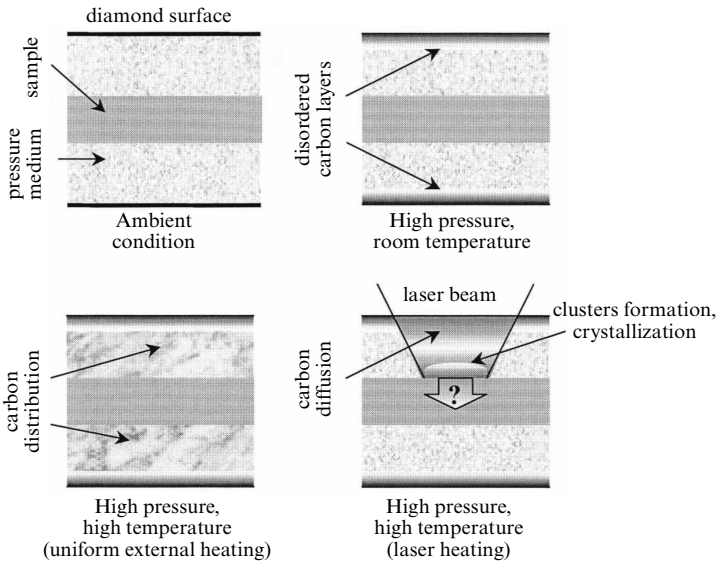


**Figure 8.** Schematic illustration of carbon diffusion and cluster formation in a DAC under different conditions.

(diamond in the given case); instead a mixture of detectable phases should form for different chemical compositions of the samples. For example, the influence of substrate (or nucleating center) on the formation of various types of carbon phases under different conditions is well documented (Knight and White 1989).

The most interesting observation from our point of view is carbon diffusion in experiments on metallic pieces compressed inside a pressure medium (figure 6). In this case, there were no direct contacts between diamond anvils and heated samples. We do not know exactly the thickness of the carbon layer formed on the metals. However, estimations could be made based on the intensity of the Raman bands. Amorphous carbon films of different thickness were deposited by the vacuum arc technique on polished silicon wafers. An ALPHA-STEP 200 profilometer was used for thickness measurements of a step that was formed by a thin mask during deposition process. We found that with our Raman spectrometers, we could detect the Raman signal if the thickness of the carbon layer was more than 20 nm which is consistent with the data of Campbell et al (1992). With an increase of layer thickness the intensity of Raman signals also increases. Comparison of intensities of Raman bands obtained from carbon films of known thicknesses with those from all samples in our experiments shows that in laser-heated DACs carbon layers 100 to 1000 nm thick were formed.

Let us estimate the time needed to form a layer about 1 μm thick at a high concentration gradient using the free atom model. A simple estimate of time necessary for the formation of a carbon layer inside the sample can be made by using Fick's first law (Lasaga 1998). Diffusive flux $J$ is proportional to the gradient of concentration $C$

$$J = -D\frac{\partial C}{\partial x} ,$$

where $x$ is the distance measured perpendicularly to the reference surface, and $D$ is the diffusion coefficient.

For example, taking as a model case of carbon diffusion in iron for which the diffusion coefficient of carbon $D$ of $1.1 \times 10^{-6}$ cm$^2$ s$^{-1}$ at 1000 K (Lasaga 1998) yields flux $J$ to be $1.1 \times 10^{19}$ atoms cm$^{-2}$ s$^{-1}$ at a distance $x$ of 10 μm and concentration of carbon atoms $C$ of $10^{22}$ atoms cm$^{-2}$. With such parameters a carbon layer with a

thickness of 1 μm could form in just 0.1 s. This means that diffusion could be the main reason of carbon transport inside the pressure chamber of the DAC under high-pressure – high-temperature conditions.

## 6 Conclusions

We have demonstrated that there are carbon phases (detected in originally carbon-free samples) in the DAC after high-pressure – high-temperature experiments, and that diamond anvils are the source of carbon. Non-hydrostatic compression at room temperature results in the formation of a polycrystalline graphite phase on the surface of samples (or at the diamond – sample interface). The temperature-induced formation of carbon phases (amorphous, diamond, graphite) was observed in a number of experiments as listed in table 1. Carbon transport in the pressure chamber of the DAC was proved by Raman signals collected from samples that were separated from diamond anvils with pressure-transmitting medium materials.

The variety of conditions used in the experiments suggests that carbon diffusion inside the pressure chamber of a DAC is a common phenomenon. This, therefore, makes it very important for high-pressure DAC research in general. The presence of carbon around or inside samples can significantly change the kinetics of phase transformations and conditions of chemical reactions (Hillgren et al 2000; Wood 1993). For example, the melting temperature obtained from laser-heating experiments in a DAC should be corrected by taking into account the possible presence of a carbon layer. The presence of a carbon phase could also be a source of discrepancies between experimental data on melting temperatures obtained for the same material by different groups and methods (shock wave, multi-anvil, and DAC). Physico-chemical properties of materials, such as element partitioning, phase transformations, chemical reactions, and resistivity, under high-pressure – high-temperature conditions should be analyzed by taking account of possible carbon transport in the DAC.

**Acknowledgments.** The facility used for this study at the Uppsala Lab was supported by the Swedish Science Foundation (NFR). The authors thank Dr J Lindgren for providing the Raman equipment. This work is supported by NSF-EAR 0001149 and 0229987. GSECARS sector is supported by NSF (Earth Sciences, Instrumentation and Facilities Program) and DOE (Geoscience Program).

**References**

Bassett W A, 2001 *Rev. Sci. Instrum.* **72** 1270 – 1272
Bundy F P, Bassett W A, Weathers M S, Hemley R J, Mao H K, Gocharov A F, 1996 *Carbon* **34** 141
Campbell A J, Heinz D L, Davis A M, 1992 *Geophys. Res. Lett.* **19** 1061 – 1064
Dubrovinsky L S, Saxena S K, 1999 *High Temp. – High Press.* **31** 385 – 391
Dubrovinsky L S, Dubrovinskaia N A, Abrikosov I A, Vennström M, Westman F, Carlson S, van Schilfgaarde M, Johansson B, 2001 *Phys. Rev. Lett.* **86** 4851 – 4854
Eremets M, 1996 *High Pressure Experimental Methods* (New York: Oxford University Press) pp 287 – 378
Ferrari A C, Robertson J, 2000 *Phys. Rev. B* **61** 14095 – 14107
Fominski V Yu, Markeev A M, Nevolin V N, Prokopenko V B, Triphonov A Yu, 1993 *Vacuum* **44** 873 – 877
Gogotsi Y G, Kailer A, Nickel K G, 1999 *Nature* **401** 663 – 664
Hillgren V J, Gessmann C K, Li J, 2000, in *Origin of the Earth and Moon* Eds R M Canup, K Righter (Tucson, AZ: University of Arizona Press) pp 245 – 263
Jamieson J C, Lawson A W, Nachtrieb N D, 1959 *Rev. Sci. Instrum.* **30** 1016
Kailer A, Nickel K G, Gogotsi Y G, 1999 *J. Raman Spectrosc.* **30** 939 – 946
Knight D S, White W B, 1989 *J. Mater. Res.* **4** 385 – 393
Lasaga A C, 1998 *Kinetic Theory in the Earth Sciences* (Princeton, NJ: Princeton University Press)
Mao H K, Hemley R J, 1991 *Nature* **351** 721 – 724
Pasternak M P, Rozenberg G Kh, Machavariani G Yu, Naaman O, Taylor R D, Jeanloz R, 1999 *Phys. Rev. Lett.* **82** 4663 – 4666

Pickard C D O, Davis T J, Wang W N, Steeds J W, 1998 *Diamond Relat. Mater.* **7** 238 – 242
Prokopenko V B, Dubrovinsky L S, Dmitriev V, Weber H P, 2001 *J. Alloys Compd.* **327** 87 – 95
Ree F H, Winter N W, Glosli J N, Viecelli J A, 1999 *Physica B* **265** 223 – 229
Rekhi S, Dubrovinsky L S, Saxena S K, 1999 *High Temp. – High Press.* **31** 299 – 305
Schindler T L, Vohra Y K, 1995 *J. Phys. Condens. Matter.* **7** L637 – L642
Shen G, Rivers M, Wang Y, Sutton S, 2001 *Rev. Sci. Instrum.* **72** 1273 – 1282
Wilhelm H, Lelaurain M, McRae E, 1998 *J. Appl. Phys.* **84** 6552 – 6558
Vohra Y K, McCauley T S, 1993 *Diamond Relat. Mater.* **3** 1087 – 1090
Weir C E, Lippincott E R, Van Valkenburg A, Bunting E N, 1959 *J. Res. Natl. Bur. Stand.* **63** 55
Wood B J, 1993 *Earth Planet. Sci. Lett.* **117** 593 – 607